Facet Formation in the Negative Quenched Kardar-Parisi-Zhang Equation

H. Jeong†, B. Kahng‡, and D. Kim†
†*Center for Theoretical Physics and Department of Physics, Seoul National University, Seoul 151-742, Korea*
‡*Department of Physics and Center for Advanced Materials and Devices, Kon-Kuk University, Seoul 143-701, Korea*

The quenched Kardar-Parisi-Zhang (QKPZ) equation with negative non-linear term shows a first order pinning-depinning (PD) transition as the driving force F is varied. We study the substrate-tilt dependence of the dynamic transition properties in 1+1 dimensions. At the PD transition, the pinned surfaces form a facet with a characteristic slope s_c as long as the substrate-tilt m is less than s_c. When $m < s_c$, the transition is discontinuous and the critical value of the driving force $F_c(m)$ is independent of m, while the transition is continuous and $F_c(m)$ increases with m when $m > s_c$. We explain these features from a pinning mechanism involving a localized pinning center and the self-organized facet formation.

PACS numbers: 68.35.Fx, 05.40.+j, 64.60.Ht

The pinning-depinning (PD) transition by an external driving force has been of much interest recently. Typical examples are interface growth in porous media under external pressure [1], dynamics of a domain wall under random fields [2,3], dynamics of a charge density wave under an external field [4], and vortex motion in superconductors under external current [5,6]. In the PD transition, there exists a critical value F_c of the driving force F, such that when $F < F_c$, interface (or charge, or vortex) is pinned by disorder, while for $F > F_c$, it moves with a constant velocity v. The velocity v plays the role of order parameter in the PD transition, which typically behaves as

$$v \sim (F - F_c)^{\theta}. \tag{1}$$

Recently, several stochastic models for the PD transition of interface growth in disordered media have been introduced [7,8]. It is believed that the models in 1+1 dimensions are described by the quenched Kardar-Parisi-Zhang (QKPZ) equation for the surface height h,

$$\partial_t h = \nu \partial_x^2 h + \frac{\lambda}{2}(\partial_x h)^2 + F + \eta(x,h), \tag{2}$$

where ν and λ are constants and the noise η depends on position x and height h with the properties of $\langle \eta(x,h) \rangle = 0$ and $\langle \eta(x,h)\eta(x',h') \rangle = 2D\delta(x-x')\delta(h-h')$. The QKPZ equation for $\lambda > 0$ exhibits a PD transition with $\theta \sim 0.64$. The surface at F_c can be described by the directed percolation (DP) cluster spanned perpendicularly to the surface growth direction in 1+1 dimensions. The roughness exponent α of the interface is given as the ratio of the two correlation length exponents of the DP cluster, that is $\alpha = \nu_\perp/\nu_\parallel \approx 0.63$. The coefficient λ of the non-linear term renormalizes to λ_r which scales as $\lambda_r \sim (F - F_c)^{-\phi}$ ($\phi \sim 0.64$). This is obtained by measuring the substrate-tilt dependence of the velocity

$$v(F,m) \sim v(F,0) + \frac{\lambda_r}{2} m^2 \tag{3}$$

where m is the tilt of the initial substrate [9].

Origin of the non-linear term in the QKPZ equation is different from that of the thermal KPZ equation with noise $\eta(x,t)$ [10]. For the quenched case, the non-linear term is induced by the anisotropic nature of disordered media, while for the thermal case, it is induced by the lateral growth effect and is proportional to the velocity of the interface which vanishes at the threshold of the PD transition [11]. In particular, Tang et al. [10] showed in the context of vortex dynamics that the effective pinning strength takes the form $(\Delta_h + s^2\Delta_x)^{2/3}/(1+s^2)^{2/3}$ where $s = \partial_x h$ is the local slope and $\Delta_h^{1/2}$ and $\Delta_x^{1/2}$ are the amplitudes of random forces in the h and x directions, respectively. When the medium is anisotropic, $\Delta_h \neq \Delta_x$ in general and the effective pinning strength depends on the local slope and generates the non-linear term in Eq.(2) with $\lambda \propto (\Delta_h - \Delta_x)$. Therefore when $\Delta_h < \Delta_x$, i.e. when the surface is driven along the easy direction, λ is negative.

The negative QKPZ equation, i.e. the QKPZ equation with negative λ is first studied in [12]. In marked contrast to the $\lambda > 0$ case, the negative QKPZ equation describes a first order transition in the sense that the velocity v shows a discontinuous jump at the PD transition. This is shown in Fig.1. At the PD transition, the pinned surface takes the shape of a mountain with flat inclination as shown in Fig.2. To elucidate the transition mechanism of the negative QKPZ equation, we study in this work the substrate-tilt dependence of the dynamic properties. We performed the direct numerical integration of Eq.(2) in one dimension with the discretized version used in [12]:

$$\begin{aligned} h(x,t+\Delta t) = h(x,t) + \Delta t\{ & h(x-1,t) + h(x+1,t) \\ & -2h(x,t) + \frac{\lambda}{8}(h(x+1,t) - h(x-1,t))^2 + F\} \\ & +(\Delta t)^{2/3}\xi(x,[h(x,t)]), \end{aligned} \tag{4}$$

where $[\cdots]$ denotes the integer part, and ξ is uniformly distributed in $[-\frac{1}{2}, \frac{1}{2}]$. The prefactor $(\Delta t)^{2/3}$ of the noise term arises from approximately coarse-graining the noise $\eta(x,h)$ during a time interval Δt. This is different from that used in Ref. [13], but does not alter physical property of the PD transition. We choose $\Delta t = 0.01$ and use the initial condition $h(x,0) = mx$ and the helicoidal boundary condition $h(L+i,t) = h(i,t) + Lm$. Numerical results are discussed below in detail.

First, we measure the critical driving force F_0 and the facet slope at m=0 (no tilt) for several values of λ. F_0 is numerically defined as the value of F at which no surface in the sample of upto 200 configurations is pinned until a large fixed time $t_0 \sim 10^6 \Delta t$. Just below F_c, at least a finite fraction of the ensemble is pinned at t_0 showing the facet morphology. The facet slope is determined by sample averages of 100 configurations. Measured values of F_0 and s_c are shown in Table 1 for $\lambda = -0.5, -1, -1.5$ and -2. Also shown are v_0, the velocity at F_0, i.e. the velocity discontinuity at the first order PD transition. Next, we examine the tilt-dependence of the surface growth. For small tilts, the first order nature of the PD transition and the morphology of the pinned surfaces at the transition do not change. Moreover, within our numerical accuracies, both the critical driving force and the critical facet slope are independent of the tilt m. We find this is so as long as m is less than a critical tilt m_c which is essentially the same as the facet slope s_c. When m becomes larger than s_c, the surfaces at the pinned state cannot form a facet with slope s_c by the helicoidal boundary condition and instead align along the substrate. In this case, the critical driving force $F_c(m)$ has to increase with m to compensate for the tilt-force. The schematic phase diagram in the $F - m$ plane is shown in Fig.3. The positively moving phase is bounded by a horizontal line at $F = F_0$ for $m < m_c$ and a smooth curve $F_c(m)$ for $m > m_c$. The transition to the $v < 0$ phase (the lower curve in Fig.3) is the continuous PD transition of directed percolation universality class. This region is better understood by rewriting the QKPZ equation in term of $h' \equiv -h$ as

$$\partial_t h' = \nu \partial_x^2 h' - \frac{\lambda}{2}(\partial_x h')^2 - F + \eta(x,h'). \qquad (5)$$

The above equation implies that the negative QKPZ equation with negative F is equivalent to the positive QKPZ equation with positive F and vice versa. The negative velocity phase in $F > 0$ region of Fig.3 can be understood as a result of the positive QKPZ equation driven by a negative force which is not strong enough to overcome the effect of the positively driving non-linear term. We confine our discussion to the upper curve of Fig.3 below.

A typical data set for the velocity as a function of F and m in the positively moving phase is shown in Fig.4, while Fig.5 shows a three dimensional plot of v versus F and m. At $F = F_0$ and for $m < m_c$, v exhibits a discontinuous jump by $\delta v(m)$. The lowest curve in Fig.4 shows this. Since $\delta v(m)$ vanishes at m=m_c, the point (F=F_0,m=m_c) may be regarded as a tricritical point in analogy with the equilibrium critical phenomena. Following [9], we measure λ_r by fitting the curves $v(F,m)$ to Eq.(3) for small m. Since it is insensitive to F, we define λ_r as that obtained from $F = F_0$;

$$\delta v(m) \equiv v(F_0, m) = v_0 - \frac{|\lambda_r|}{2} m^2 + \cdots. \qquad (6)$$

The fifth column of Table 1 shows λ_r. For F larger than but close to F_0, $v(F,0)$ is linear in F. This together with Eq.(6) allows one to approximate $v(F,m)$ as

$$v(F,m) = v_0 + A(F - F_0) - \frac{|\lambda_r|}{2} m^2 + \cdots \qquad (7)$$

where A is a constant. Setting $v = 0$ in Eq.(7), one obtains an approximate form for $F_c(m)$ as

$$F_c(m) \sim F_0 + \frac{|\lambda_r|}{2A}(m^2 - m_c^2) \qquad (8)$$

with $m_c = (2v_0/|\lambda_r|)^{1/2}$. However, for larger m, v deviates from Eq.(7) and higher order terms in m become significant. To find $F_c(m)$ and m_c more accurately, we fit the velocity curve for large m and estimate $F_c(m)$ independently from the condition of $v(F_c(m), m) = 0$. This is justified since $\theta = 1$ generically for $m \neq 0$ [10]. In Fig.6, we show the values of $F_c(m)$ obtained in this way. The relation $F_c(m_c) = F_0$ then gives an independent estimate of m_c which is also shown in Table 1. Note that m_c obtained in this way agrees well with the facet slope s_c as mentioned above. The values of m_c itself strongly depends on λ and could be fitted to a power law as $m_c \sim |\lambda|^{-0.37}$ as shown in Fig.7. Thus when $\lambda = 0$, m_c becomes infinite, which recovers the previous result that the critical force $F_c(m)$ is independent of the substrate-tilt in the quenched Edwards-Wilkinson universality class [10,9]. On the other hand, $|\lambda_r|$ scales as $|\lambda|^{0.8}$ in Fig.7 and hence $m_c \sim |\lambda|^{-0.37} \sim |\lambda_r|^{-0.46}$. This is to be compared with the zeroth order expression $m_c \sim |\lambda_r|^{-0.5}$ in Eq.(8).

In order to understand the origin of the discontinuous PD transition for $\lambda < 0$, we examine the noise distribution on the perimeter sites of critically pinned surfaces. It is found that the noise strengths around the site at the valley in Fig.2 are relatively small, corresponding to large pinning strengths. Meanwhile, when $\lambda < 0$, surfaces tend to form a flat facet to make the term $(\lambda/2)(\partial_x h)^2$ negatively large, leading to a large pinning strength. However, the curvature force $\nabla^2 h$ is almost zero on the hillside, but is positive at the valley. Thus the sites around the valley are pinned by balancing the driving forces due to the curvature and the external force F with the pinning forces due to the noise and the non-linear term. Once

the sites around the valley is pinned, the stable slope s_c of facet is selected in a self-organized way: Suppose that a surface is formed with a facet of slope $s < s_c$. Then the velocity of the sites on the hillside would be positive according to Fig.4 The pinning strength due to $(\lambda/2)s^2$ is not strong enough to resist the external force, and the sites on the hillside move upward, and tend to make the slope of the facet larger. When the slope becomes larger than s_c, however, the non-linear term is too strong, and the sites on the hillside move downward reducing the slope. Thus the slope s_c becomes stable, and surfaces form a facet with the slope s_c as shown in Fig.2. Since the surface pinning is initiated at the sites around the valley, once the pinning site is broken by an external force which is slightly bigger than F_0, the surface grows with a finite velocity, leading to the first order transition. On the other hand, when $\lambda > 0$, the non-linear term is positive, and enhances the external driving force. Thus surfaces do not form a facet. The surface pinning is mainly due to local noise strengths as can be pictured in the DP cluster. Thus the pinned sites are not localized but scattered all over the system, so that the PD transition is continuous.

It would be interesting to observe the tilt-dependence of the negative quenched KPZ equation from a stochastic model. The Sneppen A model [12,14] is known to belong to the negative QKPZ universality class. In the Sneppen A model, the restricted solid-on-solid (RSOS) condition is imposed on the height difference of neighboring columns. Because of this restriction, the surface tilt cannot be larger than a maximum value. If the maximum tilt is less than the critical slope $s_c(\lambda)$ of the stochastic model, the tricritical behavior would not be observed in simulations because the coefficient λ is not controllable. Recently a PD transition similar to the negative QKPZ equation is found in a seemingly different system, the driven Frenkel-Kontorova model [15], where the PD transition is also discontinuous and the displacement at the pinned state looks like Fig.2. However, the tricritical behavior has not been studied yet in this system.

In summary, we have investigated the tilt-dependent behavior of the negative quenched QKPZ equation. We observed and explained that there exists a characteristic substrate-tilt m_c such that the PD transition is discontinuous (continuous) when the substrate-tilt m is less (greater) than m_c. The characteristic tilt m_c is found to be the same as the facet slope s_c of the critically pinned surfaces which are formed in self-organized way and depends on the non-linear term coefficient λ as $m_c \sim |\lambda|^{-0.37}$. Moreover, the threshold force F_c for the PD transition is independent of m for $m < m_c$ and increases with increasing m for $m > m_c$. The effective non-linear term coefficient λ_r remains finite as F approaches F_c.

We would like to thank M. Kardar for suggesting this problem and F.-J. Elmer for sending Ref. [15]. This work was supported in part by the KOSEF through the SRC program of SNU-CTP, and in part by the Ministry of Education, Korea (97-2409).

[1] M.A. Rubio, C.A. Edwards, A. Dougherty, and J.P. Gollub, Phys. Rev. Lett. **63,** 1685 (1989); D. Kessler, H. Levine, and Y. Tu, Phys. Rev. A **43,** 4551 (1991).
[2] R. Bruinsma and G. Aeppli, Phys. Rev. Lett. **52,** 1547 (1984).
[3] R. Bausch, V. Dohm, H. K. Janssen, R. K.P.Zia, Phys. Rev. Lett. **47** 1837 (1981).
[4] G. Grüner, Rev. Mod. Phys. **60**, 1129 (1988).
[5] D.S. Fisher, M.P.A. Fisher, and D.A. Huse, Phys. Rev. B **43**, 130 (1991).
[6] D. Ertas and M. Kardar, Phys. Rev. Lett. **73**, 1703 (1994) ; Phys. Rev. B **53**. 3520 (1996).
[7] S.V.Buldyrev, A.-L. Barabási, F. Caserta, S. Havlin, H.E. Stanley and T. Viscek, Phys. Rev. A **45**, R8313 (1992).
[8] L.-H. Tang and H. Leschhorn, Phys. Rev. A **45** R8309 (1992).
[9] L. A. Amaral, A.-L. Barabási, and H.E. Stanley, Phys. Rev. Lett. **73,** 62 (1994).
[10] L.-H. Tang, M. Kardar, and D. Dhar, Phys. Rev. Lett. **74**, 920 (1995).
[11] M. Kardar, G. Parisi and Y. Zhang, Phys. Rev. Lett. **56,** 889 (1986).
[12] H. Jeong, B. Kahng, and D. Kim, Phys. Rev. Lett. **77,** 5094 (1996).
[13] Z. Csahók, K. Honda, and T. Vicsek, J. Phys. A **26,** L171 (1993).
[14] K. Sneppen, Phys. Rev. Lett. **69,** 3539 (1992).
[15] T. Strunz and F.-J. Elmer (cond-mat/9805288).

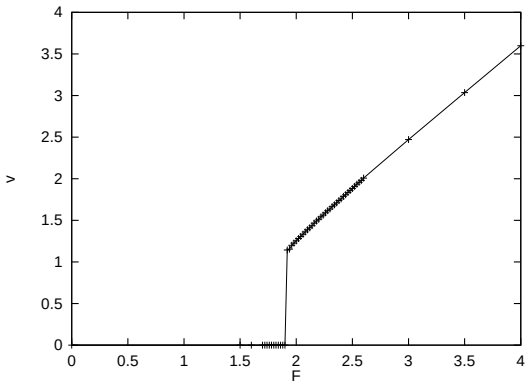

FIG. 1. The velocity versus force to show the first order transition. The data are obtained from a flat substrate with $\lambda = -0.5$. The solid line is a guide to the eye.

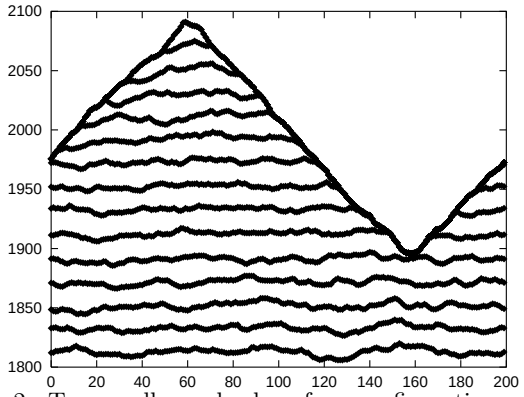

FIG. 2. Temporally evolved surface configurations of the QKPZ equation with $\lambda = -0.5$ in 1+1 dimensions at the pinning-depinning transition point. Each curve is the surface profile at constant time intervals. The facet slope is $s_c \approx 2.1$.

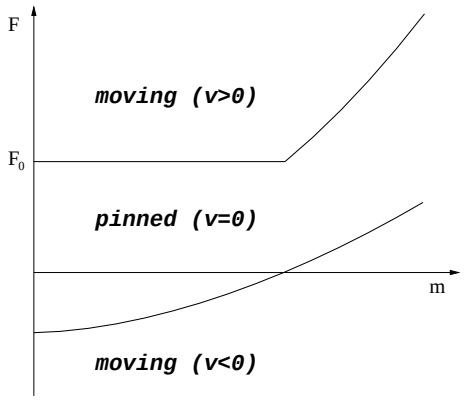

FIG. 3. The phase diagram in the F-m plane.

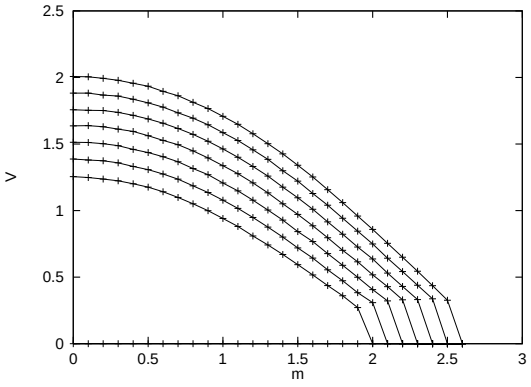

FIG. 4. The velocity versus the substrate-tilt m for several external driving forces F for the case of $\lambda = -0.5$. The curve at the bottom corresponds to the magnitude of the velocity jump at the critical force F_0, which becomes zero at a characteristic slope m_c.

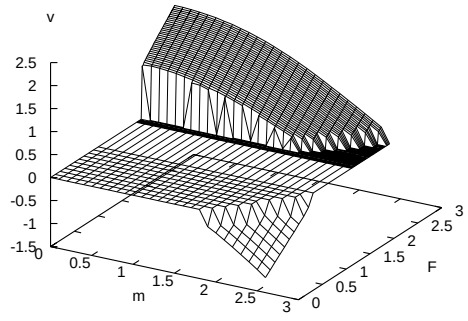

FIG. 5. Three dimensional plot of the velocity versus substrate-tilt m and external force F for the case of $\lambda = -0.5$.

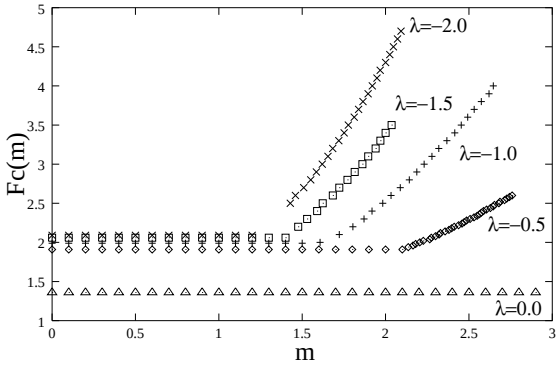

FIG. 6. The depinning critical $F_c(m)$ versus the substrate-tilt m for several values of λ.

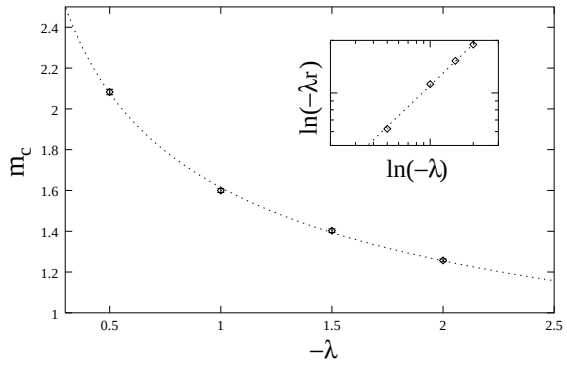

FIG. 7. Estimated numerical data for the critical tilt m_c versus λ. The broken line $m_c \sim |\lambda|^{-0.37}$ is a least square fit. Inset: The λ-dependence of λ_r showing $|\lambda| \sim |\lambda_r|^{0.8}$.

TABLE I. Measured values of the critical driving force F_0, the facet slope s_c, the velocity discontinuity v_0, the effective non-linear parameter λ_r, and the critical substrate-tilt m_c.

λ	F_0	s_c	v_0	λ_r	m_c
-0.5	1.91	2.08	1.20	-0.62	2.11

-1.0	1.99	1.60	1.30	-1.12	1.64
-1.5	2.06	1.40	1.35	-1.52	1.39
-2.0	2.09	1.26	1.42	-1.89	1.24